A New Unbalanced Voltage Compensation Method Based on HOPF Oscillator for Three-Phase DC/AC Inverters With Unbalanced Loads

Luo, Siyi; Wu, Weimin; Koutroulis, Eftichios; Chung, Henry Shu-hung; Blaabjerg, Frede

Published in:
I E E E Transactions on Smart Grid

DOI (link to publication from Publisher):
10.1109/TSG.2022.3184911

Publication date:
2022

Document Version
Accepted author manuscript, peer reviewed version

A New Unbalanced Voltage Compensation Method based on Hopf Oscillator for Three-Phase DC/AC Inverters with Unbalanced Loads

Siyi Luo, Weimin Wu, *Member, IEEE*, Eftichis Koutroulis, *Senior Member, IEEE*, Henry Shu-Hung Chung, *Fellow, IEEE*, and Frede Blaabjerg, *Fellow, IEEE*

***Abstract*—In islanded microgrids, distributed generators (DGs) are employed as distributed compensators to improve the power quality on the load side. Due to the access of unbalanced loads, the low-voltage microgrid will naturally exhibit three-phase unbalance, which may cause additional power losses and deteriorate power quality. Therefore, this paper proposes a novel unbalanced-voltage compensation control method based on the Hopf oscillator, which introduces the negative-sequence voltage and current into the traditional Hopf oscillator to achieve the negative sequence voltage droop characteristics. It can not only realize the negative sequence droop control of a single inverter, but it is also capable to support the reactive power automatic distribution between multi-parallel grid-forming inverters. Compared with the traditional unbalanced voltage compensation method based on filtered negative sequence reactive power, the proposed unbalanced voltage compensation method can slightly improve the dynamic response. Experimental results verify the effectiveness of the proposed control strategy.**

Keywords*— *Grid-forming inverters, Hopf oscillator, unbalanced-voltage compensation.

I. Introduction

Distributed power generation systems have been widely used because they enable the efficient and flexible use of renewable energy. Microgrids consist of distributed generators (DGs), energy conversion devices, loads, and small autonomous power generation and distribution systems with self-control, self-protection, and self-management capabilities [1],[2]. Microgrid features two operational modes: grid-connected operation and islanded operation, and can be smoothly switched between these two modes [3],[4]. When the microgrid operates in the islanded mode, if three-phase unbalanced loads exist in the power system (mainly through the single-phase load connections between two phases, or between a single-phase and the neutral conductor) an undesired unbalanced voltage will be generated, which will adversely affect the overall power system and the interconnected equipment. Therefore, the International Electrotechnical Commission (IEC) recommends limiting voltage unbalance in electrical systems to less than 2% [5].

In order to compensate for the unbalanced voltage, the unbalanced voltage compensation control strategy can be applied to voltage source inverters (VSIs) [6]. For a microgrid with multiple VSI-based DGs, the compensation effort should be shared among multiple VSIs. In [7]-[9], the central controllers of microgrid collects the voltages at the point of common coupling (PCC), and then transmits the unbalanced voltage compensation command signal to DG via the communication link. In [10], the central secondary controller sends appropriate compensation signals to the DG local controller to compensate for the unbalanced voltage at the PCC in an islanded microgrid. However, the compensation effect is limited by low-bandwidth communication links. In order to reduce the dependence on communication, the relationship between negative sequence reactive power and negative sequence voltage is used to automatically compensate for the unbalanced voltage between DGs, while sharing the compensation work [11]-[13]. However, the response speed of the compensation effect will be compromised by the filtered measurement data. In [14], by adjusting the negative sequence output impedance of the DG itself, the voltage unbalance factor of the inverter output voltage can be improved. However, when the interconnection line impedances are different, the negative sequence current cannot be well shared between DGs. In [15], a distributed cooperative negative sequence current sharing method with dynamic consensus algorithm has been introduced. Only one communication link is needed between adjacent DGs, and no dedicated central controller is needed to achieve satisfactory compensation of the unbalanced voltages. In case of networked microgrids, the control of the negative sequence current between microgrids is a key issue. Aiming at the problem of power distribution error under unbalanced loads, a new hierarchical control method is proposed in [16], which can realize the precise distribution of single-phase current without data exchange between distributed energy sources. An unbalanced load current not only causes unbalanced voltage, but also adversely affects the performance of traditional current limiting mechanisms. Model-predictive control was combined with the *V-I* droop method in [17] to minimize the unbalanced voltage, increase

Manuscript received October 28, 2021; revised April 12, 2022; accepted June 16, 2022. Date of publication; date of current version. This work was supported in part by the National Natural Science Foundation of China under Grant 51877130, in part by the National Key Research and Development Project of China under Grant 2017YFGH001164 and in part by the program "Bilateral and Multilateral Research & Technology Co-operation between Greece and China" under Grants 2017YFGH001164 and eSOLAR/T7ΔΚΙ-00066. Recommended for publication by Associate Editor *****. (Corresponding author: Weimin Wu.)

Siyi Luo and Weimin Wu are with the Electrical Engineering Department, Shanghai Maritime University, Shanghai 201306, China (e-mail: luosiyi@stu.shmtu.edu.cn; wmwu@shmtu.edu.cn;).

E. Koutroulis is with the School of Electrical and Computer Engineering, Technical University of Crete, Chania 73100, Greece (e-mail: efkout@electronics.tuc.gr).

H. S.-H. Chung is with the Department of Electrical Engineering and the Centre for Smart Energy Conversion and Utilization Research, City University of Hong Kong, Hong Kong (e-mail: eeshc@cityu.edu.hk).

F. Blaabjerg is with the Energy Engineering Department, Aalborg University, Aalborg 9100, Denmark (e-mail: fbl@et.aau.dk).

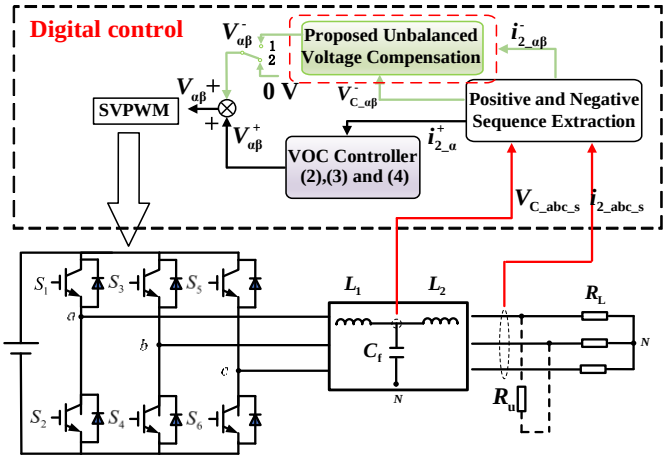

Fig. 1. VOC-based three-phase inverter with the proposed unbalanced-voltage compensation method under unbalanced load.

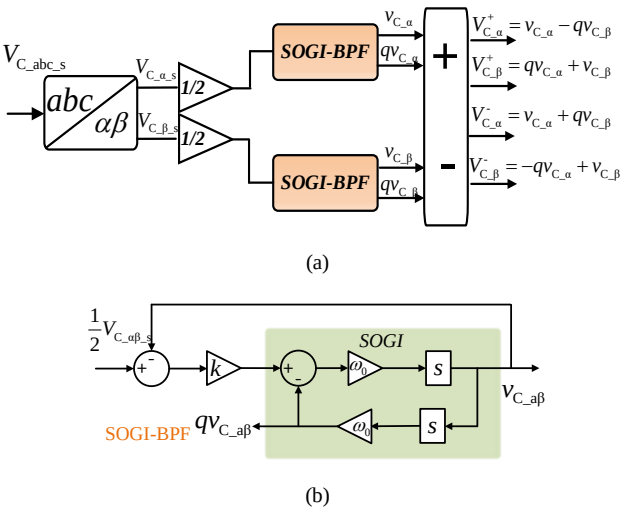

Fig. 2. Structure of positive and negative sequence extraction module.

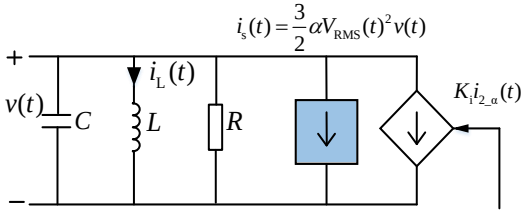

Fig. 3. The equivalent circuit structure of a VOC controller.

current limit, and prevent active power overloading. However, this method does not provide zero sharing error and might give rise to relatively high values of voltage unbalance. A mixed-integer nonlinear programming model is used in the islanded–mode of operation of a microgrid in [18] to optimize power flow during unbalanced three-phase voltage operating conditions.

The droop characteristics between negative sequence reactive power and negative sequence voltage can be used for compensation of the unbalanced voltage. The Hopf oscillator controller as a grid-forming controller has been applied to three-phase parallel islanded inverters. It controls the inverter output voltage to emulate drooping behavior, faster response, and better robustness [19]-[21]. It is worth noting that the voltage synchronization part of the Hopf oscillator can synchronize the output voltage of the oscillator with any external voltage. Therefore, through a reasonable design, the Hopf oscillator can output a proper negative sequence voltage to achieve compensation of the unbalanced voltage.

In this paper, a new method of unbalanced-voltage compensation based on the Hopf oscillator is proposed for three-phase DC/AC inverter to compensate the unbalanced voltages caused by the unbalanced loads. Specifically, by introducing a negative sequence component into the traditional Hopf oscillator, the droop characteristics between the negative sequence reference voltage and the negative sequence reactive power are realized, thereby autonomously compensating the negative sequence voltage and reactive power of the inverter. Compared with the traditional unbalanced voltage compensation method that relies on filtered negative sequence reactive power [11]-[13], the proposed unbalanced voltage control method can improve the dynamic response speed.

The rest of the paper is organized as follows. In Section II, the operation of the VOC-based three-phase three-wire inverter under unbalanced load is introduced. Then, in Section III, the principle of unbalanced voltage compensation is explained in detail, and the proposed negative sequence Hopf oscillator is introduced to achieve unbalanced-voltage compensation. In Section IV, the effectiveness of the proposed Hopf-oscillator-based unbalanced-voltage compensation method is demonstrated by using a three-phase three-wire experimental prototype system. Finally, the conclusions are summarized and the future potential is discussed in Section V.

II. Unbalanced Voltage Caused by Unbalanced Loads of Three-Phase Inverter

In this paper, three-phase three-wire unbalanced islanded inverters are addressed. Since there is no zero-sequence current in a three-wire ungrounded electrical system [22], the zero-sequence voltage drop will not affect the system voltage. Droop control and VOC were the primary controllers that simulate the droop characteristics of synchronous generators to achieve power sharing [23]-[29]. Due to fast dynamics and low harmonic content, VOC is select as the primary control in this paper.

Fig. 1 depicts the VOC-based three-phase inverter with unbalanced load and the proposed control strategy. The power stage consists of a DC power supply, inverter and LCL filter. The LCL filter is used to attenuate the high frequency harmonics introduced by the SVPWM operation. The inverter-side inductor and grid-side inductor of the LCL filter are denoted by L_1 and L_2, respectively. The capacitor between the two inductors is denoted by C_f. A balanced star-connected three-phase load, R_L, is connected to the inverter output, and a single-phase load, R_u, is connected between phases *a* and *b* to emulate common unbalanced loading conditions. When the proposed unbalanced voltage compensation module is activated, the SPDT switch is switched to position 1. The positive and negative sequence extraction in this paper is based on SOGI-BPF [30]. The structure of positive and negative sequence extraction module is shown in the Fig. 2. The transfer function of SOGI-BPF $B(s)$ is shown in (1). By setting reasonable k and ω_0, $v_{C_\alpha\beta}$will be equal to the fundamental frequency

This article has been accepted for publication in IEEE Transactions on Smart Grid. This is the author's version which has not been fully edited and content may change prior to final publication. Citation information: DOI 10.1109/TSG.2022.3184911

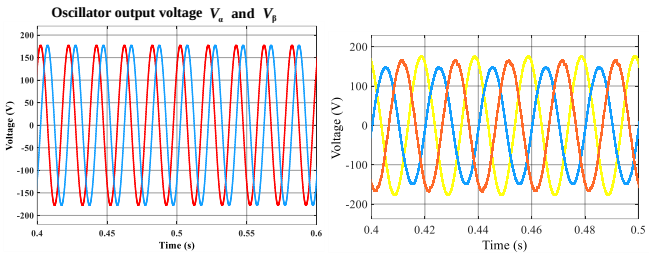

(a) (b)

Fig. 4. Simulation results: (a) oscillator output voltage and (b) unbalanced inverter output voltage.

component of $0.5V_{C\_\alpha\beta}$, and $qv_{C\_\alpha\beta}$ will be the quadrature component of $0.5V_{C\_\alpha\beta}$, where, $q=e^{-j\frac{\pi}{2}}$.

$$B(s)=\frac{v_{C\_\alpha\beta}}{0.5V_{C\_\alpha\beta\_s}}(s)=\frac{k\omega_0 s}{s^2+k\omega_0 s+\omega_0^2} \tag{1}$$

Similarly, $i_{2_\alpha}^{-}$and$i_{2_\alpha\beta}^{+}$ can also be obtain from $i_{2\_abc\_s}$ with positive and negative sequence extraction module.

Virtual oscillator control is an emerging nonlinear time-domain controller applied to microgrids, which can control the dynamic response of a DC/AC inverter to emulate the limit-cycle oscillator, thereby achieving power sharing and frequency support in the islanded mode of operation. The equivalent circuit structure of a VOC is shown in Fig. 3. The Kirchhoff's equations of VOC are as follows:

$$L\frac{di_L(t)}{dt}=v(t) \tag{2},$$

$$C\frac{dv(t)}{dt}=-i_s(t)+\sigma v(t)-i_L(t)-K_i i_{2\_\alpha}(t) \tag{3},$$

where, L and C represent the oscillator inductance and capacitance, respectively, which are used to generate the resonant frequency. The oscillator resistor is expressed as R, where R = -1/σ, which is related to the response speed of the oscillator. Also, i_s(t) represents the controlled current source related to the oscillator output voltage. By designing a suitable controlled current source i_s(t), the oscillator can exhibit a faster response speed and lower harmonic content [31]. The current flowing through the inductor L can be represented by i_L(t), and the voltage across the oscillator capacitor is represented by v(t). It is worth noting that the positive sequence output current of the inverter, $i_{2\_\alpha}^{+}$, multiplied by the adjustable gain factor, K_i, is introduced in the VOC in order to achieve better droop characteristics of the oscillator. The positive sequence reference voltages, $V_{\alpha\beta}^{+}$, generated by the VOC are calculated as follows:

$$\begin{aligned} V_\alpha^+ &= K_v\cdot v(t)=\sqrt{2}V_{RMS}(t)\cos(\omega t+\theta(t)) \\ V_\beta^+ &= K_v\cdot \omega L * i_L(t) \end{aligned} \tag{4},$$

where:

$$V_{RMS}(t)=\left(\frac{\sigma\pm\sqrt{\sigma^2-6\alpha K_i/K_v\bar{P}(t)}}{3\alpha}\right)^{\frac{1}{2}} \tag{5},$$

$$\omega=\omega^*+\frac{K_i K_v\bar{Q}(t)}{2CV_{RMS}^2(t)} \tag{6},$$

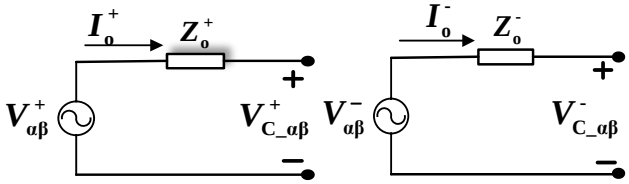

Fig. 5. Equivalent positive and negative sequence circuits.

and K_v is the voltage scale gain, while $\bar{P}$ and $\bar{Q}$ are the average active and reactive power output of the inverter. The design of VOC-based controllers has been sufficiently studied in the literature [26], and will not be discussed more in this paper.

However, VOC, as a grid-forming control method, mainly focuses on the balanced systems. Therefore, when a VOC-controlled inverter is connected to an unbalanced system, due to the absence of a suitable unbalanced voltage compensation strategy, the inverter output voltage will be severely unbalanced, deteriorating the quality and reliability of the inverter output power. When the traditional VOC-based inverter is connected to an unbalanced load, the output reference voltage of the oscillator is shown in Fig. 4(a), and the output voltage of the inverter is shown in Fig. 4(b). Although the output voltage of the virtual oscillator is a pair of symmetrical voltages, the three-phased voltages output by the inverter are unbalanced.

III. Proposed Unbalanced-Voltage Compensation Method Based on Hopf-Oscillator

When the inverter is connected to unbalanced loads, it will produce unbalanced output voltage and current. The symmetrical component method is an effective method to analyze the three-phase unbalance of the power system. The basic idea is to decompose the three-phase unbalanced current and voltage into three symmetrical positive-sequence phasors, negative-sequence phasors, and zero-sequence phasors, so that the power system unbalance problem can be transformed into an equivalent balanced system problem for further processing.

A. Principle of Unbalanced-Voltage Compensation

As mentioned above, the zero-sequence component is not addressed in this paper. The positive and negative sequence equivalent circuits of the three-phase inverter can be simplified as shown in Fig. 5, where the inverter output voltage is equal to the voltage across the capacitor $V_{C\_\alpha\beta\_s}$ since L_2 can be seen as part of the line impedance. Among them, the positive sequence reference voltage $V_{\alpha\beta}^{+}$ can be obtained through VOC. Z_o^+ is the positive sequence output impedance of the inverter and Z_o^- is its negative sequence output impedance. I_o^+ and I_o^- are the positive-sequence and negative-sequence output currents of the inverter, respectively. The inverter output voltage, $V_{C\_\alpha\beta\_s}$, can be obtained by adding the positive-sequence output voltage $V_{C\_\alpha\beta}^{+}$ and the negative-sequence output voltage $V_{C\_\alpha\beta}^{-}$, as follows:

$$V_{C\_\alpha\beta\_s}=V_{C\_\alpha\beta}^{+}+V_{C\_\alpha\beta}^{-} \tag{7},$$

where, the negative-sequence output voltage of the inverter $V^{-}_{C\_\alpha\beta}$ can be derived as:

$$V^{-}_{C\_\alpha\beta} = V^{-}_{\alpha\beta} - I^{-}_{o} * Z^{-}_{o} \quad (8),$$

When there is no additional module for compensation of the unbalanced voltage, the SPDT switch is set to position 2, it holds that $V^{-}_{\alpha\beta} \approx 0$. Therefore, if the control system can generate a suitable negative-sequence reference voltage $V^{-}_{\alpha\beta}$, the negative-sequence voltage at the output of the inverter can be reduced. To this end, the positive-sequence voltage and the negative-sequence voltage can be controlled separately. The positive-sequence voltage can be controlled by a traditional VOC, while the negative-sequence voltage is controlled by the additional unbalanced-voltage compensation module. In this paper, only the positive-sequence components are introduced into the VOC to achieve better positive-sequence power sharing, while the negative-sequence components are used for compensation of the unbalanced voltage.

B. Unbalanced Voltage Compensation Realization Using Hopf-Oscillator

In this paper, a Hopf-based unbalanced-voltage compensation strategy is proposed to improve the voltage unbalance factor (VUF) of the inverter output voltage.

The Hopf oscillator is a common nonlinear oscillator with a stable limit cycle in the state-space. In other words, for any non-zero initial state, the oscillator can generate a stable periodic oscillation signal. Compared with the virtual oscillator, the Hopf oscillator can produce a more ideal limit cycle, it is not easily affected by the initial state, and can recover from external disturbances in a short time. In [19] and [21], the traditional Hopf oscillator has been successfully applied to the parallel operation of microgrid inverters. In order to realize power distribution between parallel inverters, a current sharing term is introduced in the traditional Hopf oscillator, and a voltage pre-synchronization term is introduced at the same time, so that the output voltage of the nonlinear oscillator is automatically synchronized with the inverter terminal voltage. Its form is as follows:

$$\dot{V}_{\alpha} = \mu(V^{2}_{ref} - V^{2}_{\alpha} - V^{2}_{\beta})V_{\alpha} - \omega V_{\beta} + k_{v}V_{c\alpha} - k_{i}i_{\alpha} \quad (9),$$

$$\dot{V}_{\beta} = \mu(V^{2}_{ref} - V^{2}_{\alpha} - V^{2}_{\beta})V_{\beta} + \omega V_{\alpha} + k_{v}V_{c\beta} - k_{i}i_{\beta} \quad (10).$$

where, V_{ref}, μ and ω are oscillator parameters, which are used to adjust the dynamic characteristics of the oscillator. The μ is used to characterize the speed at which the oscillator converges to the limit cycle. ω characterizes the oscillator frequency. V_{ref} is used to characterize the rated amplitude of the oscillator output voltage, that is, the radius of the limit cycle, k_v is the voltage gain and k_i is the current gain. $V_{c\alpha}$ and $V_{c\beta}$ are the voltage pre-synchronization term. i_{α} and i_{β} are the power sharing item. Among them, $V_{c\alpha}$, $V_{c\beta}$, i_{α} and i_{β} include positive sequence component and negative sequence component, and the positive sequence component is much larger than the negative sequence component. Therefore, the negative sequence output voltage $V^{-}_{\alpha\beta}$of the traditional Hopf oscillator is too small to compensate for the unbalanced voltage.

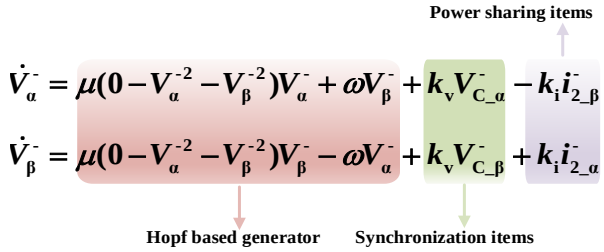

Fig. 6. The proposed unbalanced-voltage compensation module based on Hopf oscillator.

In order to solve the issue of alleviating the voltage unbalance, a new Hopf oscillator with negative sequence reference voltage output is proposed for three-phase unbalanced inverters in islanded mode, to achieve droop characteristic between the negative sequence reactive power Q^{-} and negative sequence reference voltage $V^{-}_{\alpha\beta}$. The structure of the proposed Hopf-based unbalanced voltage compensation module is shown in Fig. 6, where, $V^{-}_{\alpha} = V^{-}\sin(\theta)$, $V^{-}_{\beta} = V^{-}\cos(\theta)$, $V^{-}_{C\_\alpha} = V^{-}_{C}\sin(\theta)$, $V^{-}_{C\_\beta} = V^{-}_{C}\cos(\theta)$, $i^{-}_{2\_\alpha} = i^{-}\cos(\theta)$, $i^{-}_{2\_\beta} = i^{-}\sin(\theta)$, where V^{-} is the negative-sequence reference voltage amplitude of the oscillator, V^{-}_{C} is the negative-sequence capacitor voltage amplitude, and i^{-} is the negative-sequence output current amplitude of the inverter. V^{-}_{α} and V^{-}_{β} together form the negative-sequence reference voltages $V^{-}_{\alpha\beta}$ added to the positive sequence reference voltages $V^{+}_{\alpha\beta}$ generated by the VOC. $V^{-}_{C\_\alpha}$ and $V^{-}_{C\_\beta}$ are the inverter negative-sequence output voltage pre-synchronization items to automatically synchronize the negative-sequence output voltage of the Hopf oscillator with the inverter terminal negative-sequence voltage.

In order to produce a droop characteristic between the negative-sequence reference output voltage of the proposed Hopf oscillator and the negative-sequence reactive power of the inverter, negative-sequence currents, $i^{-}_{2\_\alpha}$ and $i^{-}_{2\_\beta}$, are introduced into the proposed Hopf oscillator. In order to prevent the unbalance compensation module from generating a negative sequence voltage when balancing the load, V_{ref} is set to 0 V. According to Fig. 6, the phase dynamic equations of the proposed Hopf-based negative-sequence voltage oscillator can be derived as follows:

$$\dot{V}^{-} = -\mu(V^{-})^{3} + k_{v}V^{-}_{C} + k_{i}(i^{-}_{2\_\alpha}\cos\theta - i^{-}_{2\_\beta}\sin\theta) \quad (11),$$

$$\dot{\theta} = \omega - \frac{k_{i}}{V^{-}}(i^{-}_{2\_\alpha}\sin\theta + i^{-}_{2\_\beta}\cos\theta) \quad (12).$$

Using the concept of period average can further simplify and analyze the weakly nonlinear periodic dynamics in (11) and (12). Similar to droop control, the V^{-} and Q^{-} relations can be derived as follows:

$$\begin{aligned}\dot{V}^{-} &= -\mu(V^{-})^{3} + k_{v}V^{-}_{C} + k_{i}(i^{-}_{2\_\alpha}\cos\theta - i^{-}_{2\_\beta}\sin\theta) \\ &= -\mu(V^{-})^{3} + k_{v}V^{-}_{C} - \frac{2}{3V^{-}_{C}}k_{i}Q^{-}\end{aligned} \quad (13).$$

The positive roots of amplitude equation in (13) are solved as:

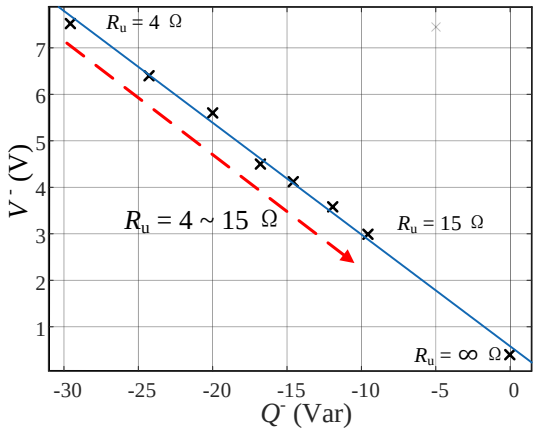

Fig. 7. Measured value of steady-state output negative-sequence reference voltage amplitude of the proposed Hopf oscillator V^- and negative-sequence reactive power Q^-.

$$V^- = \sqrt[3]{\frac{k_v V_C^- - \frac{2k_i Q^-}{3V_C^-}}{\mu}} \tag{14}$$

As shown in (14), there is a similar droop relationship between the amplitude of the negative-sequence reference voltage amplitude of the oscillator, V^-, and the negative-sequence reactive power of the inverter, Q^-, which is used to compensate for the unbalanced voltage. Simulation results reported in Fig. 7 are obtained by changing the single-phase load R_u between 0 and 15 Ω. In each case, the negative sequence voltage, and the negative sequence power at the output of the steady-state inverter were recorded. The best-fit linear model (plotted as a solid line) based on the measured data (plotted as ×) is shown in Fig. 7, which proves that the negative sequence voltage amplitude negative sequence reactive power droop law is embedded in the output negative sequence reference voltage of the proposed Hopf oscillator. It is worth noting that R_u = ∞ Ω illustrates proposed unbalanced voltage control work during the normal balanced operation, the amplitude of the negative sequence reference voltage of the oscillator, $V^- \approx 0$ V, which is also in line with the purpose of setting $V_{ref} = 0$ V.

According to the superposition theorem in circuit theory, the three-phase circuit can also be decomposed into two circuits of positive and negative sequence, respectively, for further analysis. The positive and negative sequence circuits of the three-phase inverter can be simplified as shown in Fig. 5.

Before the unbalanced-voltage compensation module is activated, the SPDT switch is in position 2, it holds that $V_{\alpha\beta}^- = 0$ V. Hence, the negative sequence output voltage of the inverter, $V_{C\_\alpha\beta}^-$, can be derived as:

$$V_{C\_\alpha\beta}^- = -I_o^- * Z_o^- \tag{15}$$

When the unbalance compensation module is activated, the SPDT switch is switched to position 1, the negative sequence output voltage of the inverter, V_C^-, can also be derived as:

$$V_C^- = \sqrt[3]{\frac{k_v V_C^- - \frac{2k_i Q}{3V_C^-}}{\mu}} - I_o^- * Z_o^-$$
$$\Rightarrow \left| \sqrt[3]{\frac{k_v V_C^- - \frac{2k_i Q}{3V_C^-}}{\mu}} - I_o^- * Z_o^- \right| < \left| -I_o^- * Z_o^- \right| \tag{16}$$

Since the first term in (16) is higher than 0, the negative sequence output voltage amplitude of the inverter is reduced compared to its value before the module for compensation of the voltage unbalance is activated.

C. Parameter Selection

μ is the damping coefficient that affects the speed of the oscillator's time transient response. Its selection is based on engineering experience [19]. It is worth noting that to prevent over-compensation of the negative sequence output voltage of the inverter, the values of k_i and k_v should be selected in an appropriate range.

Considering the frequency droop characteristics of the negative sequence output voltage of the oscillator and the negative sequence voltage compensation effect, k_i should be selected according to (17). In addition, k_v should be selected according to the VUF of the system. If k_v is too large or too small, the inverter will be over-compensated or under-compensated. In this paper, k_v is selected under the condition that the VUF does not exceed 8%, that is, before the unbalanced voltage compensation module is activated, the maximum possible unbalanced voltage ($I_o^- * Z_o^-$) of the inverter does not exceed 13 V.

$$k_i \le \frac{\Delta\omega_{max} V^-}{(i_{2\_\alpha}^- \sin\theta + i_{2\_\beta}^- \cos\theta)} \tag{17}$$

$$I_o^- * Z_o^- - 2\% * V^+ < \sqrt[3]{\frac{k_v V_C^- - \frac{2k_i Q^-}{3V_C^-}}{\mu}} < I_o^- * Z_o^- \tag{18}$$

The maximum frequency deviation is defined as $\Delta\omega_{max}$ = 1%*ω, according to (17), the selection range of k_i can be obtained, $k_i \le 1$. When the system is in a steady state, the voltage unbalance factor of the inverter system does not exceed 2%, so $V_C < 2\% * V^+$. Therefore, the selection range of k_v can be obtained according to (18), $3000 \le k_v \le 9000$. In addition, the influence of the control parameters on the stability of the negative sequence control system is analyzed by the small-signal dynamic model.

When the Hopf oscillator is in steady state, (12), (13) can be written as (19) and (20), where, V_{eq}^- is the oscillator output voltage amplitude at steady state

$$\dot{V}_{eq}^- = -\mu (V_{eq}^-)^3 + k_v V_{C\_eq}^- + \sqrt{2} k_i i_q^- \tag{19}$$

$$\dot{\theta} = \omega - \frac{\sqrt{2} k_i}{V_{eq}^-} i_d^- \tag{20}$$

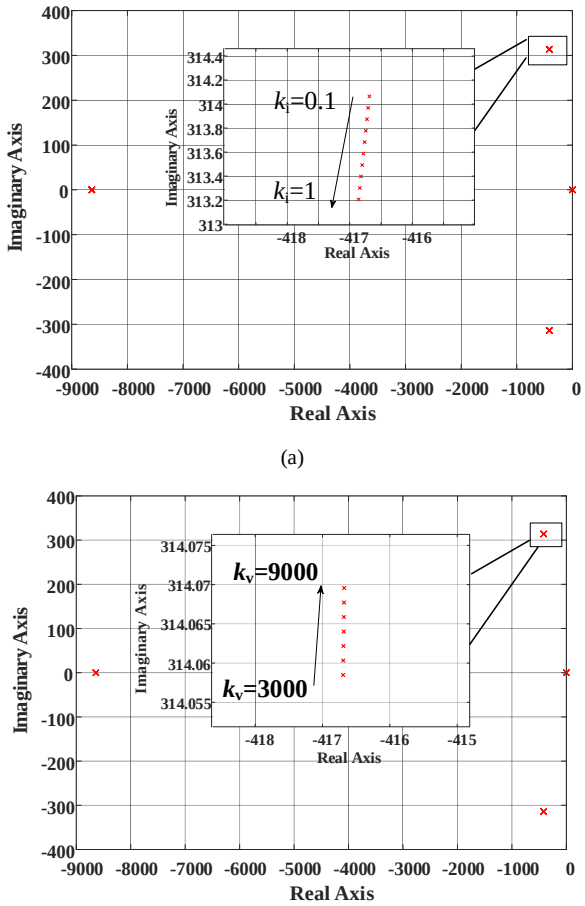

Fig. 8. Root locus diagrams for (a) $0.1 \le k_i \le 1$, (b) $3000 \le k_v \le 9000$.

In this paper, the LCL filter is simplified to the L-type filter analysis, so the state equations of the inverter negative sequence output current and the inverter negative sequence output voltage can be written as:

$$\dot{i}_d^- = -\frac{R}{L} * i_d^- - \omega i_q^- + \frac{\sqrt{2}}{L}(V_{eq}^- - V_{C\_eq}^-) \quad (21),$$

$$\dot{i}_q^- = -\frac{R}{L} * i_q^- + \omega i_d^- + \frac{\sqrt{2}}{L}(-V_{C\_eq}^-) \quad (22).$$

Select $\Delta X = [\Delta V_{eq}^- \ \Delta\theta \ \Delta i_d^- \ \Delta i_q^-]$ as the state vector, the small-signal model is compactly represented as $\Delta\dot{X}=A\Delta X$, where

$$A = \begin{bmatrix} -3\mu\left(V_{eq}^-\right)^2 & k_v V_{C\_eq}^- & 0 & \sqrt{2}k_i \\ \dfrac{k_i\sqrt{2}i_d^-}{\left(V_{eq}^-\right)^2} & 0 & -\dfrac{k_i\sqrt{2}}{V_{eq}^-} & 0 \\ \dfrac{\sqrt{2}}{L} - \dfrac{k_i\sqrt{2}i_d^- i_q^-}{\left(V_{eq}^-\right)^2} & -\dfrac{\sqrt{2}V_{C\_eq}^-}{L} & -\dfrac{R}{L} - \dfrac{k_i\sqrt{2}i_q^-}{V_{eq}^-} & \dfrac{k_i\sqrt{2}i_d^-}{V_{eq}^-} - \omega^* \\ \dfrac{k_i\sqrt{2}(i_d^-)^2}{\left(V_{eq}^-\right)^2} & -\dfrac{\sqrt{2}V_{C\_eq}^-}{L} & \omega^* - \dfrac{k_i\sqrt{2}i_d^-}{V_{eq}^-} & -\dfrac{R}{L} \end{bmatrix} \quad (23).$$

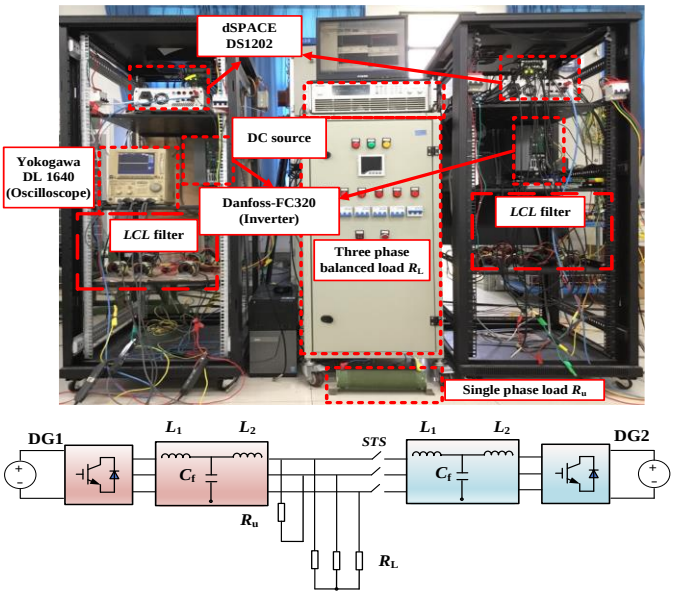

Fig. 9. Experimental setup with multiple three-phase islanded inverters.

TABLE I
SIMULATION AND EXPERIMENT PARAMETERS

Symbols	*Description*	*Value*
U_{dc}	DC bus voltage	350 V (RMS)
f ,f_s	Inverter, Switching and sampling frequency	50 Hz，10 kHz
L_1	Inverter side inductor	1.2 mH
C	Filter capacitor	6 uF
L_2	Grid side inductor	1.2 mH
L	Oscillator inductor	52.087 μH
C	Oscillator capacitor	0.1945 F
R	Oscillator resistance	-10.7962 Ω
α	Current source coefficeint	7.1975
K_i	Current feedback gain	0.152
K_V	Voltage scaling factor	110
R_L	Balanced loads	20 Ω

The influences of parameters k_v, and k_i are discussed as below. As is shown in Fig. 8, when k_v and k_i increase, the eigenvalues of the Jacobian matrix A move slightly, which means that the parameters k_v and k_i are not sensitive to the stability of the system. Hence, the resulting values of the operational parameters are the following: ω=2*50*π, μ=20, k_i = 1 and k_v =6000.

IV. Experimental Verification

In order to demonstrate the effectiveness of the proposed unbalanced-voltage compensation method based on the Hopf oscillator, the parallel three-phase inverter shown in Fig. 9 is used as a test system. In case #1, the STS is in the OFF state, and only inverter #1 is connected to the unbalanced load. In case #2, the STS is in the ON state and the parallel inverter is connected to the unbalanced load to verify the effectiveness of the proposed method. A single-phase load R_u is connected between phases *a* and *b* to simulate the unbalanced loading conditions. The dSPACE DS1202 platform with Danfoss-FC320 is used to emulate the control and inverter systems,

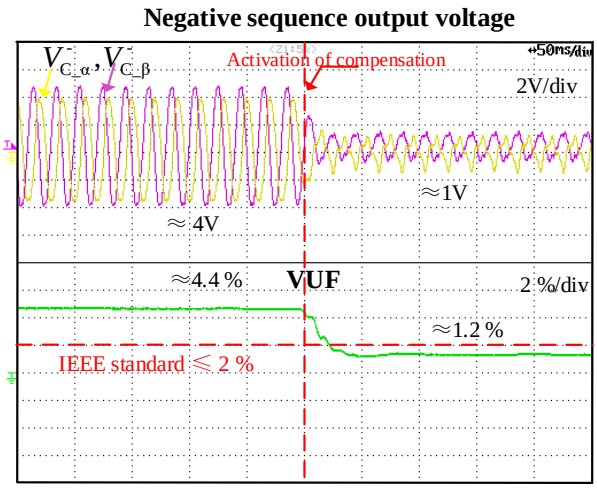

Fig. 10. Negative sequence inverter output voltage and VUF value for test case #1.

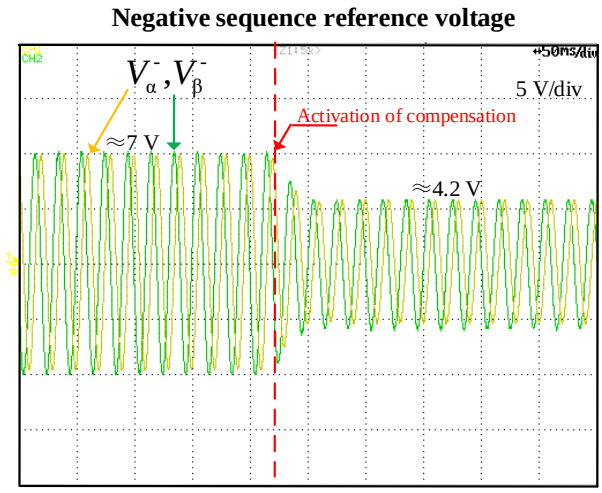

Fig. 11. Negative sequence reference voltage for test case #1.

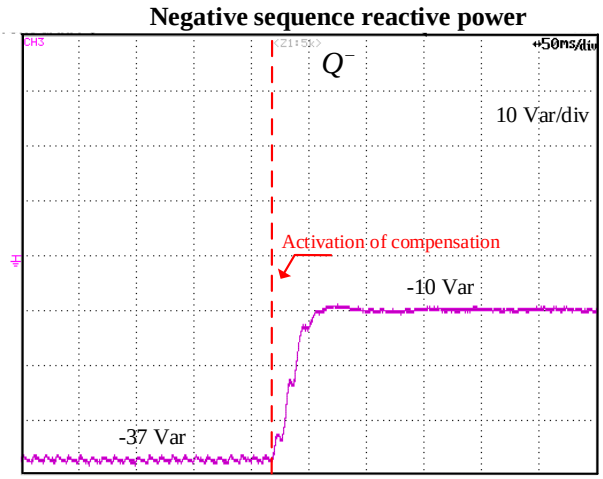

Fig. 12. Negative sequence reactive power for test case #1.

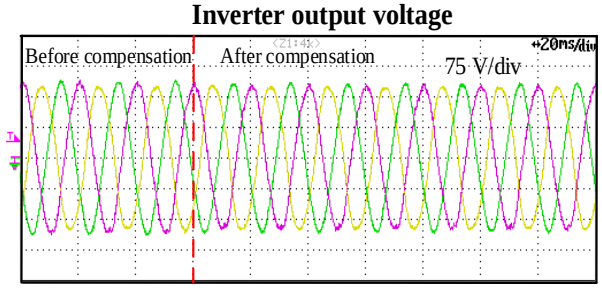

Fig. 13. Three-phase voltage of the inverter for test case #1.

respectively. The specific parameters of the experimental platform and the parameters of the controller are listed in Table I. The Chroma 62150H-600S is used to provide DC power output.

A. Case 1: Unbalanced-Voltage Compensation Realization with a Single Three-Phase Inverter

In this case, in order to simulate an unbalanced load, a 5 Ω single-phase resistive load R_u is connected in series between phases *a* and *b*. In this paper, the voltage unbalance factor is considered as the index of unbalance [32], which is defined as follows:

$$VUF = \frac{V^-_{RMS}}{V^+_{RMS}} * 100 \tag{24}$$

where V^-_{RMS} and V^+_{RMS} are the RMS values of the negative sequence voltage and positive sequence voltage, respectively.

The negative-sequence output voltage waveform of the inverter and the resulting experimental value of VUF are shown in Fig. 10. The purple and yellow curves are the inverter negative-sequence output voltages, and the green curve is the experimentally measured VUF value. It is worth noting that in order to clearly show the compensation effect, the control module for compensation of the unbalanced voltage was suddenly connected to the control system. As shown, before the unbalanced-voltage compensation module is activated, the value of the negative-sequence output voltage of the inverter is high, which causes the voltage unbalance factor to exceed the limit defined in the IEEE standards (i.e. 2 %) [33], [34]. After the unbalanced-voltage compensation module is suddenly connected to the control system, the negative sequence voltage produced by the inverter was reduced significantly after 0.05 s, successfully improving the value of the VUF of the inverter output voltage to less than 1.2 %. Similarly, the inverter output negative sequence voltage is also significantly reduced.

The negative sequence reference output voltage of the Hopf oscillator (green and yellow curves) is shown in Fig. 11. Before the unbalanced-voltage compensation module is connected to the control system, the Hopf oscillator has generated the reference voltage according to (14). It is worth noting that at this time, the SPDT switch in position 2, the Hopf oscillator has not been connected to the control system, that is, the negative sequence reference voltage generated by the Hopf oscillator are not added to the positive sequence reference voltage $V^+_{\alpha\beta}$ generated by the virtual oscillator. After the SPDT switch is set to position 1, the proposed unbalanced voltage compensation module is connected to the control system, by compensating for the unbalanced voltage (lower negative sequence voltage), Q^- and the negative sequence reference voltage produced by the Hopf oscillator are reduced. The inverter output negative-sequence reactive power (purple curve) is shown in Fig. 12. As shown in Fig. 12. The inverter output negative sequence reactive power is reduced from -37 Var to -10 Var after the inverter three-phase output voltages are compensated. This is consistent with the negative sequence voltage compensation principle

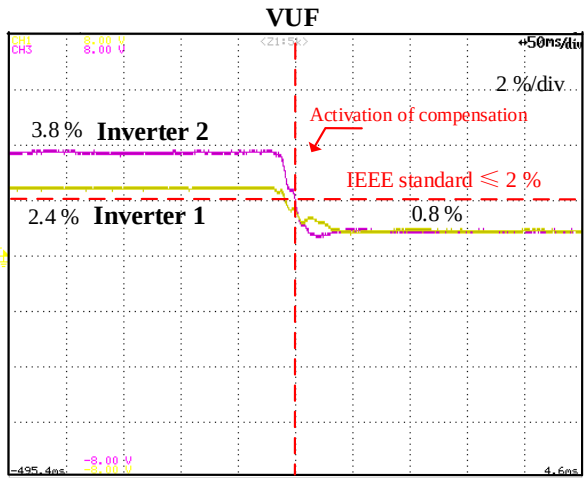

Fig. 14. The VUF of the inverter for test case #2.

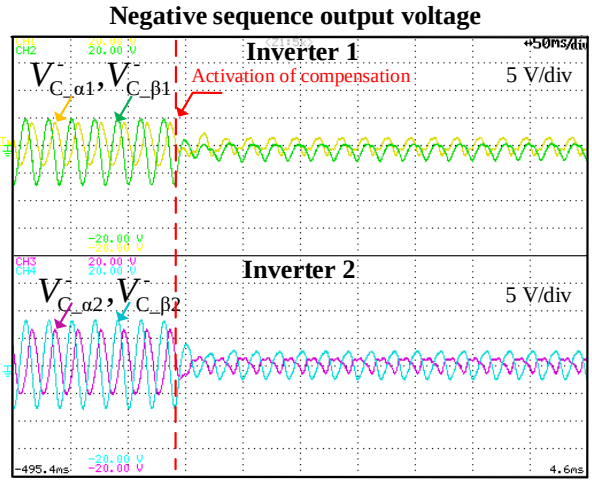

Fig. 15. Negative sequence voltage of the inverter for test case #2.

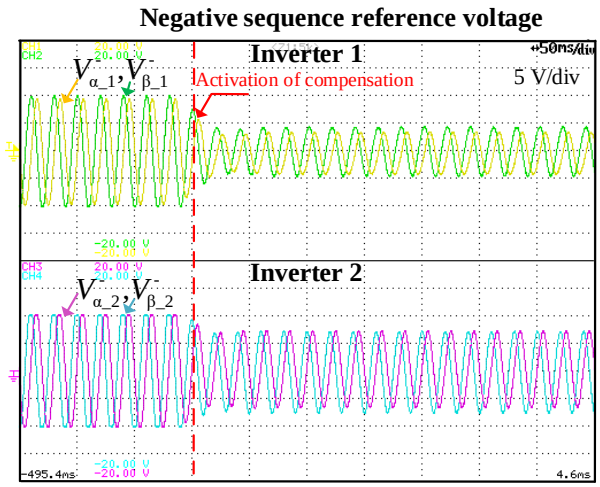

Fig. 16. Negative sequence reference voltage for test case #2.

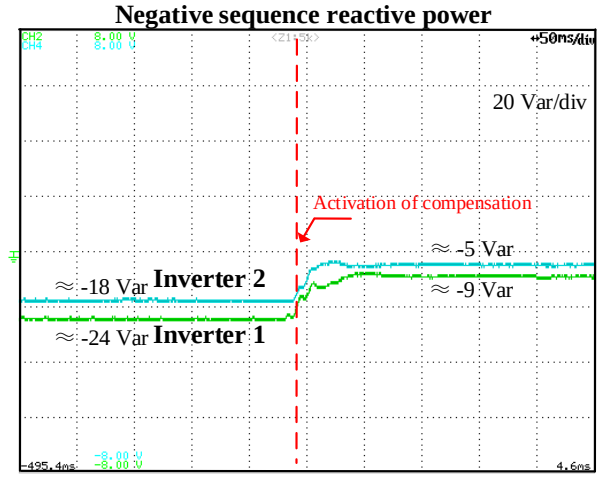

Fig. 17. Negative sequence reactive power of the inverter for test case #2.

expressed by (14). Fig. 13 shows the measured three phase output voltages of the inverter. These figures demonstrate the effectiveness of the proposed method in compensating the unbalanced output voltage of the inverter.

B. Case 2: Negative Sequence Reactive Power Distribution between of Multi-Parallel Grid-Forming Inverters

In this case, the STS in Fig. 9 is set in the ON state and the parallel inverter is connected to the unbalanced load. The rated power of inverter #1 is 4000 W, and the rated power of inverter #2 is 2000 W. Also, the three-phase balanced load is R_L=100 Ω, and the single-phase load is R_u=10 Ω. In order to distribute the negative sequence reactive power among the inverters according to their nominal capacity, the negative sequence current gain of inverter #1 is set to k_i = 20, and the negative sequence current gain of inverter #2 is set to k_i = 40.

As shown in Fig. 14, the VUF of inverter #1 is reduced from 2.4% to 0.8%, and the VUF of inverter #2 is reduced from 3.8% to 0.8%, which meets the limit dictated by the IEEE standard (i.e. VUF ≤ 2 %). Thus, it is concluded that the output voltage unbalance factor of the inverter has been significantly improved. The negative-sequence voltages of inverter #1 and inverter #2 before and after compensation are shown in Fig. 15.

As the unbalanced-voltage compensation module based on Hopf oscillator is connected to the control system, the negative sequence voltages produced by the two inverters are effectively reduced. The inverter negative-sequence reference voltages produced by the Hopf oscillators of Inverter #1 (green and yellow curves) and Inverter #2 (purple and blue curves) are shown in Fig. 16. The negative sequence reference voltage decreases as the negative sequence reactive power output by the inverter decreases, which is consistent with the similar droop characteristics of the negative sequence reactive power produced by the inverter and the negative sequence reference voltage generated by the Hopf oscillator, respectively. In this way, the autonomous compensation of the voltage unbalance between the inverters is realized without communication between them. The negative sequence reactive power output of the inverter is shown in Fig. 17. It is observed that the proposed unbalanced-voltage compensation method achieves to share negative sequence reactive power according to the rated capacity of the inverters. The phase-*a* output current of the two inverters is shown in Fig. 18. It is demonstrated that the two inverters can share current according to their capacity before and after compensation.

C. Case 3: Dynamic Performance Comparison between Traditional and Proposed Unbalanced Voltage Compensation Methods

In this case, the STS is in the OFF state, the single-phase load R_u=5 Ω. The traditional unbalanced voltage compensation method is based on local measurement to create a voltage droop for the negative sequence reference

This article has been accepted for publication in IEEE Transactions on Smart Grid. This is the author's version which has not been fully edited and content may change prior to final publication. Citation information: DOI 10.1109/TSG.2022.3184911

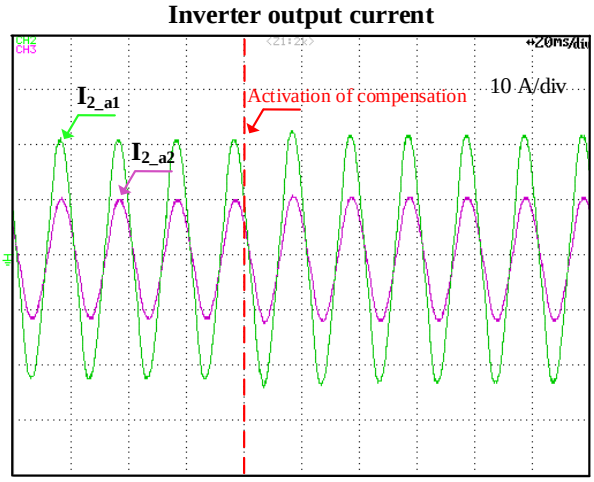

Fig. 18. Inverter output current of the inverter for test case #2.

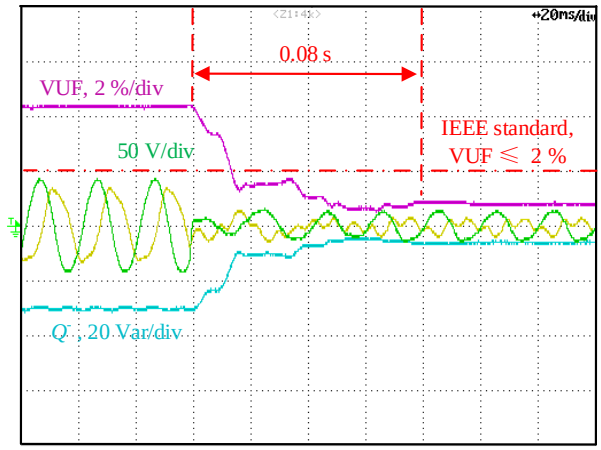

Fig. 19. Dyanmic performance of systen using the traditional unbalanced voltage compensation method.

voltage and introduce the filtered negative sequence reactive power Q^{-}_{LPF} as an imbalance indicator into the control system [11]-[13], while the primary controller adopts droop control. The filtered negative sequence reactive power Q^{-}_{LPF} can be defined by using local measurements [12], and can be defined as:

$$Q^{-}_{\mathrm{LPF}} = u_{\mathrm{rms}}\sqrt{(i_{\alpha})^2+(i_{\beta})^2} * \frac{\omega_{\mathrm{c}}}{s+\omega_{\mathrm{c}}} \quad (25),$$

where ω_{c} is the cutoff frequency of low-pass filters (LPFs), which is set to 100 (rad/s). However, due to the time needed by the LPFs to calculate Q^{-}_{LPF}, the dynamic response speed of the compensation effort is slow. The smaller the ω_{c}, the slower the response speed. The unbalance compensation reference of traditional unbalanced compensation can be defined as:

$$UCR = Q^{-}_{\mathrm{LPF}} * V_{\mathrm{o}}^{-} * K_{\mathrm{N}} \quad (26),$$

where, K_{N} is unbalance compensation gain and V_{o}^{-} is negative sequence voltage. The unbalance compensation reference *UCR* is added to the positive sequence reference voltage to achieve compensation, and the positive sequence reference voltage is generated by the droop control.

In this test, VOC is use as the primary control to generate positive sequence reference voltage, and the traditional and

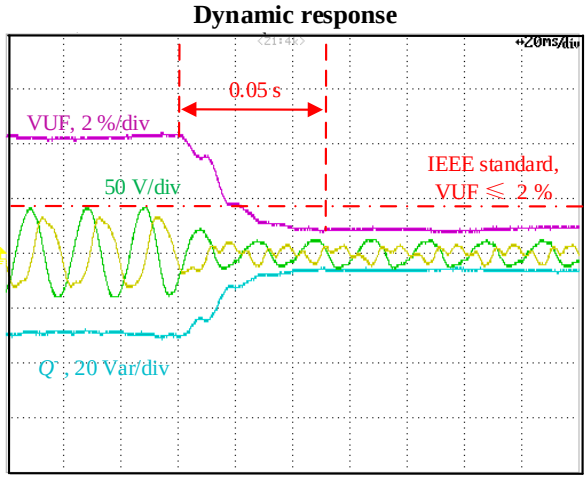

Fig. 20. Dyanmic performance of systen using the proposed unbalanced voltage compensation method.

proposed unbalanced voltage compensation methods are introduced into the control system respectively. As shown in Fig. 19, since the filtered Q^{-}_{LPF} is introduced into *UCR*, the dynamic response of the traditional unbalanced voltage compensation method is slower (about 0.08 s). The purple line is VUF of the inverter, the blue line is negative sequence reactive power, and the yellow and green line are negative sequence voltage of the inverter. However, as shown in Fig. 20, the dynamic response of the proposed unbalanced compensation method is smoother and faster (0.05 s). The experimental results show that, due to the need to measure and filter the negative-sequence reactive power, the traditional unbalanced voltage compensation method has inherent limitations in dynamic performance. In contrast, the proposed Hopf oscillator-based unbalanced voltage compensation acts on the instantaneous measured value, essentially providing a faster and better damping response.

V. Conclusions

In this paper, a new control method is proposed for VOC-based inverter systems to compensate the unbalanced output voltage caused by unbalanced loads. The overall conclusions can be summarized as follows:

1) The proposed unbalanced voltage compensation realizes reactive power versus voltage droop by introducing the negative sequence voltage and negative sequence current of the inverter into the Hopf oscillator.

2) The proposed unbalanced-voltage compensation method can compensate for voltage unbalance and automatically realize negative-sequence reactive power distribution between multi-parallel grid-forming inverters.

3) Compared with the traditional unbalanced voltage compensation method based on filtered negative sequence reactive power, the proposed unbalanced voltage compensation method shows a faster response speed.

The effectiveness of proposed method for compensation of the unbalanced voltage has been verified via an experimental laboratory setup based on the dSPACE DS1202 platform.

REFERENCES

[1] Z. Shuai, C. Shen, X. Liu, Z. Li, and Z. J. Shen, "Transient angle stability of virtual synchronous generators using Lyapunov's direct method," *IEEE Trans. Smart Grid*, vol. 10, no. 4, pp. 4648–4661, Jul. 2019.

[2] Z. Shuai,W. Huang, X. Shen,Y. Li, X. Zhang, and Z. J. Shen, "A maximum power loading factor (MPLF) control strategy for distributed secondary frequency regulation of islanded microgrid," *IEEE Trans. Power Electron.*, vol. 34, no. 3, pp. 2275–2291, Mar. 2019.

[3] J. W. Simpson-Porco, Q. Shafiee, F. Dörfler, J. C. Vasquez, J. M. Guerrero and F. Bullo, "Secondary Frequency and Voltage Control of Islanded Microgrids via Distributed Averaging," *IEEE Trans. Ind. Electron*., vol. 62, no. 11, pp. 7025-7038, Nov. 2015.

[4] M. A. Awal, H. Yu, H. Tu, S. M. Lukic and I. Husain, "Hierarchical Control for Virtual Oscillator Based Grid-Connected and Islanded Microgrids," *IEEE Trans. Power Electron.*, vol. 35, no. 1, pp. 988-1001, Jan. 2020.

[5] A. V. Jouanne and B. Banerjee, "Assessment of voltage unbalance," *IEEE Trans. Power Del.*, vol. 16, no. 4, pp. 782–790, Oct. 2001.

[6] N. R. Merrit, C. Chakraborty, and P. Bajpai, "New voltage control strategies for VSC based DG units in an unbalanced microgrid," *IEEE Trans. Sustain. Energy*., vol. 8, no. 3, pp. 1127–1139, Jul. 2017.

[7] J. He, Y. Li, and F. Blaabjerg, "An enhanced islanding microgrid reactive power, imbalance power, and harmonic power sharing scheme," *IEEE Trans. Power Electron.*, vol. 3, no. 6, pp. 3389–3401, Jun. 2015.

[8] W. Feng, K. Sun, Y. Guan, J. M. Guerrero, and X. Xiao, "Active power quality improvement strategy for grid-connected microgrid based on hierarchical control," *IEEE Trans. Smart Grid.*, vol. 9, no. 4, pp. 3486–3495, Jul. 2018.

[9] S. Acharya, M. S. El Moursi, A. Al-Hinai, A. S. Al-Sumaiti, and H. Zeineldin, "A control strategy for voltage unbalance mitigation in an islanded microgrid considering demand side management capability," *IEEE Trans. Smart Grid.*,vol. 10, no. 3, pp. 2558–2568, May 2019.

[10] M. Savaghebi, A. Jalilian, J. C. Vasquez and J. M. Guerrero, "Secondary Control Scheme for Voltage Unbalance Compensation in an Islanded Droop-Controlled Microgrid," *IEEE Trans. Smart Grid.*, vol. 3, no. 2, pp. 797-807, June 2012.

[11] M. Savaghebi, A. Jalilian, J. C. Vasquez and J. M. Guerrero, "Autonomous Voltage Unbalance Compensation in an Islanded Droop-Controlled Microgrid," *IEEE Trans. Ind. Electron*., vol. 60, no. 4, pp. 1390-1402, April 2013.

[12] Y. Han, P. Shen, X. Zhao, and J. M. Guerrero, "An enhanced power sharing scheme for voltage unbalance and harmonics compensation in an islanded AC microgrid," *IEEE Tran. Energy Convers.*, vol. 31, no. 3, pp. 1037–1050, Sep. 2016

[13] Y. Peng, Z. Shuai, J. M. Guerrero, Y. Li, A. Luo and Z. J. Shen, "Performance Improvement of the Unbalanced Voltage Compensation in Islanded Microgrid Based on Small-Signal Analysis," *IEEE Trans. Ind. Electron.*, vol. 67, no. 7, pp. 5531-5542, July 2020.

[14] M. Hamzeh, H. Karimi and H. Mokhtari, "A New Control Strategy for a Multi-Bus MV Microgrid Under Unbalanced Conditions," *IEEE Trans. Power Systems*., vol. 27, no. 4, pp. 2225-2232, Nov. 2012.

[15] L. Meng et al., "Distributed Voltage Unbalance Compensation in Islanded Microgrids by Using a Dynamic Consensus Algorithm," *IEEE Trans. Power Electron*., vol. 31, no. 1, pp. 827-838, Jan. 2016.

[16] M. S. Golsorkhi, D. J. Hill and M. Baharizadeh, "A Secondary Control Method for Voltage Unbalance Compensation and Accurate Load Sharing in Networked Microgrids," *IEEE Trans. Smart Grid.*, vol. 12, no. 4, pp. 2822-2833, July 2021.

[17] M. S. Golsorkhi and D. D. Lu, "A Decentralized Control Method for Islanded Microgrids Under Unbalanced Conditions," *IEEE Trans. Power Del.*, vol. 31, no. 3, pp. 1112-1121, June 2016.

[18] P. P. Vergara, J. C. López, M. J. Rider and L. C. P. da Silva, "Optimal Operation of Unbalanced Three-Phase Islanded Droop-Based Microgrids," *IEEE Trans. Smart Grid.*, vol. 10, no. 1, pp. 928-940, Jan. 2019.

[19] M. Li, Y. Gui, Y. Guan, J. Matas, J. M. Guerrero and J. C. Vasquez, "Inverter Parallelization for an Islanded Microgrid Using the Hopf Oscillator Controller Approach with Self-Synchronization Capabilities," *IEEE Trans. Ind. Electron.*, vol. 68, no. 11, pp. 10879-10889, Nov. 2021.

[20] M. Lu, S. Dutta, V. Purba, S. Dhople and B. Johnson, "A Grid-compatible Virtual Oscillator Controller: Analysis and Design," 2019 *IEEE Energy Conversion Congress and Exposition (ECCE)*, 2019, pp. 2643-2649.

[21] M. Li, B. Wei, J. Matas, J. M. Guerrero and J. C. Vasquez, "Advanced Synchronization Control for Inverters Parallel Operation in Microgrids Using Coupled Hopf Oscillators," *CPSS Trans. Power Electron and Applic*, vol. 5, no. 3, pp. 224-234, Sept. 2020.

[22] R. C. Dugan, M. F. McGranaghan, S. Santoso, and H.W. Beaty, *Electrical Power Systems Quality*, 2nd ed. New York: McGraw-Hill, 2003.

[23] X. Meng, J. Liu and Z. Liu, "A Generalized Droop Control for Grid-Supporting Inverter Based on Comparison Between Traditional Droop Control and Virtual Synchronous Generator Control," *IEEE Trans. Power Electron.*, vol. 34, no. 6, pp. 5416-5438, June 2019.

[24] S. Wang, Z. Liu, J. Liu, D. Boroyevich and R. Burgos, "Small-Signal Modeling and Stability Prediction of Parallel Droop-Controlled Inverters Based on Terminal Characteristics of Individual Inverters," *IEEE Trans. Power Electron.*, vol. 35, no. 1, pp. 1045-1063, Jan. 2020.

[25] H. Han, X. Hou, J. Yang, J. Wu, M. Su, and J. M. Guerrero, "Review of power sharing control strategies for islanding operation of AC microgrids," *IEEE Trans. Smart Grid*, vol. 7, no. 1, pp. 200–215, Jan. 2016.

[26] B. B. Johnson, M. Sinha, N. G. Ainsworth, F. Dörfler and S. V. Dhople, "Synthesizing Virtual Oscillators to Control Islanded Inverters," *IEEE Trans. Power Electron.*, vol. 31, no. 8, pp. 6002-6015, Aug. 2016.

[27] D. Raisz, T. T. Thai and A. Monti, "Power Control of Virtual Oscillator Controlled Inverters in Grid-Connected Mode," *IEEE Trans. Power Electron.* vol. 34, no. 6, pp. 5916-5926, June 2019.

[28] M. A. Awal, H. Yu, H. Tu, S. M. Lukic and I. Husain, "Hierarchical Control for Virtual Oscillator Based Grid-Connected and Islanded Microgrids," *IEEE Trans. Power Electron.*, vol. 35, no. 1, pp. 988-1001, Jan. 2020.

[29] M. Ali, H. I. Nurdin and J. E. Fletcher, "Dispatchable Virtual Oscillator Control for Single-Phase Islanded Inverters: Analysis and Experiments," *IEEE Trans. Ind. Electron*, vol. 68, no. 6, pp. 4812-4826, June 2021.

[30] P. Rodriguez, A. V. Timbus, R. Teodorescu, M. Liserre and F. Blaabjerg, "Flexible Active Power Control of Distributed Power Generation Systems During Grid Faults," *IEEE Trans. Ind. Electron.*, vol. 54, no. 5, pp. 2583-2592, Oct. 2007.

[31] S. Luo, W. Wu, E. Koutroulis, H. S. -H. Chung and F. Blaabjerg, "A New Virtual Oscillator Control Without Third-Harmonics Injection For DC/AC Inverter," *IEEE Trans. Power Electron.*, vol. 36, no. 9, pp. 10879-10888, Sept. 2021.

[32] R. C. Dugan, M. F. McGranaghan, S. Santoso, and H.W. Beaty, *Electrical Power Systems Quality*, 2nd ed. New York: McGraw-Hill, 2003.

[33] *IEEE Recommended Practice for Electric Power Distribution for Industrial Plants*, ANSI/IEEE Std. 141, 1993.

[34] *IEEE Recommended Practice for Monitoring Electric Power Quality*, IEEE Std. 1159, 2009.

Siyi Luo was born in Jiangxi, China, in 1996. He received the B.S. degree in software engineering and electrical engineering from East China Jiao Tong University, Nanchang, China, in 2018. He is currently working toward the M.S. degree in electrical engineering with Shanghai Maritime University, Shanghai, China. His current research interests include power electronics, distributed generation, renewable energy systems, and control of microgrid cluster systems.

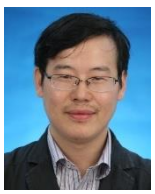

Weimin Wu (M'16) received Ph.D. degrees in Electrical Engineering from the College of Electrical Engineering, Zhejiang University, Hangzhou, China, in 2005.

He worked as a research engineer in the Delta Power Electronic Center (DPEC), Shanghai, from July, 2005 to June, 2006. Since July, 2006, he has been a Faculty Member at Shanghai Maritime University, where he is currently a Full Professor in Department of Electrical Engineering. He was a Visiting Professor in the Center for Power Electronics Systems (CPES), Virginia Polytechnic Institute and State University, Blacksburg, USA, from Sept. 2008 to March.

2009. From Nov. 2011 to Jan. 2014, he was also a visiting professor in the Department of Energy Technology, Aalborg University, Demark, working at the Center of Reliable Power Electronics (CORPE). He has coauthored over 100 papers and holds eight patents. His areas of interests include power converters for renewable energy systems, power quality, smart grid, and energy storage technology. Dr. Wu serves as an Associate Editor for the IEEE TRANSACTIONS ON INDUSTRY ELECTRONICS.

Eftichios Koutroulis (M'10–SM'15) was born in Chania, Greece, in 1973. He received the B.Sc. and M.Sc. degrees in electronic and computer engineering, in 1996 and 1999, respectively, and the Ph.D. degree in the area of power electronics and renewable energy sources (RES) from the School of Electronic and Computer Engineering, Technical University of Crete, Chania, Greece, in 2002. He is currently an Associate Professor in the School of Electrical and Computer Engineering, Technical University of Crete, where he also serves as Director of the Circuits, Sensors and Renewable Energy Sources laboratory. His research interests include power electronics, the development of microelectronic energy management systems for RES and the design of photovoltaic and wind energy conversion systems.

Henry Shu-Hung Chung (M'95-SM'03-F'16) received the B.Eng. and Ph.D. degrees in electrical engineering from the Hong Kong Polytechnic University, Kowloon, Hong Kong, in 1991 and 1994, respectively.

Since 1995, he has been with the City University of Hong Kong, where he is currently the Associate Dean (Research) of the College of Engineering, the Chair Professor with the Department of Electrical Engineering, and the Director of the Centre for Smart Energy Conversion and Utilization Research. He has edited one book, authored eight research book chapters, and over 460 technical papers, including 220 refereed journal articles in his research areas, and holds 70 patents.

Dr. Chung was the Chair of the Technical Committee of the High-Performance and Emerging Technologies, IEEE Power Electronics Society in 2010-2014. He is currently Associate Editor of the IEEE Transactions on Power Electronics and the IEEE Journal of Emerging and Selected Topics in Power Electronics. He is an Associate Editor of the IEEE Transactions on Power Electronics and the IEEE Journal of Emerging and Selected Topics in Power Electronics.

Frede Blaabjerg (S'86–M'88–SM'97–F'03) was with ABB-Scandia, Randers, Denmark, from 1987 to 1988. From 1988 to 1992, he got the PhD degree in Electrical Engineering at Aalborg University in 1995. He became an Assistant Professor in 1992, an Associate Professor in 1996, and a Full Professor of power electronics and drives in 1998. From 2017 he became a Villum Investigator. He is honoris causa at University Politehnica Timisoara (UPT), Romania and Tallinn Technical University (TTU) in Estonia.

His current research interests include power electronics and its applications such as in wind turbines, PV systems, reliability, harmonics and adjustable speed drives. He has published more than 600 journal papers in the fields of power electronics and its applications. He is the co-author of four monographs and editor of ten books in power electronics and its applications.

He has received 33 IEEE Prize Paper Awards, the IEEE PELS Distinguished Service Award in 2009, the EPE-PEMC Council Award in 2010, the IEEE William E. Newell Power Electronics Award 2014, the Villum Kann Rasmussen Research Award 2014, the Global Energy Prize in 2019 and the 2020 IEEE Edison Medal. He was the Editor-in-Chief of the IEEE TRANSACTIONS ON POWER ELECTRONICS from 2006 to 2012. He has been Distinguished Lecturer for the IEEE Power Electronics Society from 2005 to 2007 and for the IEEE Industry Applications Society from 2010 to 2011 as well as 2017 to 2018. In 2019-2020 he served as a President of IEEE Power Electronics Society. He has been Vice-President of the Danish Academy of Technical Sciences. He is nominated in 2014-2020 by Thomson Reuters to be between the most 250 cited researchers in Engineering in the world.